

# Physicochemical and osteoplastic characteristics of 3D printed bone grafts based on synthetic calcium phosphates and natural polymers

E K Nezhurina<sup>1</sup>, P A Karalkin<sup>1</sup>, V S Komlev<sup>2</sup>, I K Sviridova<sup>1</sup>, V A Kirsanova<sup>1</sup>, S A Akhmedova<sup>1</sup>, Ya D Shanskiy<sup>1</sup>, A Yu Fedotov<sup>2</sup>, S M Barinov<sup>2</sup> and N S Sergeeva<sup>1</sup>

<sup>1</sup>P.A. Hertsen Moscow Oncology Research Institute – branch of National Medical Research Radiological Center of Ministry of Health of Russian Federation, Russia, Moscow

<sup>2</sup>Baikov Institute of Metallurgy and Materials Science, Russia, Moscow

E-mail: eliznezhurina@gmail.com

**Abstract.** A creation of personalized implants for regeneration of bone tissue seems to be a very promising biomedical technological approach. We have studied the physicochemical characteristics, cyto- and biocompatibility of three-dimensional constructs based on sodium alginate and gelatin in combination with 2 types of calcium phosphate (tricalcium phosphate or octacalcium phosphate) obtained by inkjet 3D printing. In our experiments, we have studied the physical and chemical properties of the constructs – their porosity, chemical composition, microarchitecture of the surface and mechanical elasticity. The cytocompatibility of 3D constructs and matrix-for-cell properties were investigated in vitro on a model of human osteosarcoma MG-63 cell line by means of MTT assay. The biocompatibility of 3D constructs was studied on the model of subcutaneous implantation in mice up to 12 weeks. All types of 3D constructs were cytocompatible in vitro, demonstrated good matrix-for-cells properties, and had supported cell proliferation for 2 weeks. In results of subcutaneous in vivo test all constructs demonstrated biocompatibility with slow bioresorption of organic and inorganic components. Osteogenesis proceeded more actively in rat tibia model defects (marginal excision), substituted by 3D printed 3-component implants based on alginate, gelatin and octacalcium phosphate.

## 1. Introduction

The development of biomedical materials intended for bone defects replacement is still an important medical and social issue. At the present time, a number of requirements have been postulated for “ideal” biomaterial: biocompatibility, high surface area, high degree of porosity (at least 60-85%) with interconnected pores with diameters within the range of 100-1000  $\mu\text{m}$ , optimal rate of resorption (biodegradation) *in vivo*, corresponding to the rate of new bone formation, osteoconductive and, more preferable, osteoinductive properties. Finally, a biomaterial for reconstructive plastic surgery of bone tissue must provide a mechanical stiffness at the site of implantation and hold its shape during the reparative phase [1]. Many current concepts for osteoplastic materials are inspired by the structure of natural bone tissue which extracellular matrix comprises a perfect nanocomposite consisted of collagen fibrils chemically linked to carbonated apatite. In this term a different biomimetic approaches involving natural polymers and calcium phosphate (CP) ceramic were developed in last decades [2,3]. In this study we investigated the structural features, biocompatibility and osteoplastic properties of



3D-constructs based on sodium alginate, gelatin, and two types of calcium phosphates (tricalcium phosphate and octacalcium phosphate) obtained by three-dimensional printing. Being a precursor of biological apatite OCP promotes a mineralization of new bone tissue and also demonstrates convenient solubility in simulating body fluids [4,5]. Recent technologies of rapid prototyping, e.g. 3D printing, are capable of creating personalized grafts with precise geometry of the defects according to patient's CT/MRI data [6]. This was the method we chose to construct bone replacement implants.

## 2. Materials and Methods

### 2.1. Fabrication of bone grafts using 3D printing technology

The production of an experimental three-dimensional (3D) constructs was performed according to original technology (patent RF No. RU2606041C2) by using custom-designed extrusion-based 3D printer. The hydrogel ("ink") for 3D printing contained 2 % sodium alginate (CAS 9005-38-3, Acros), 10 % gelatin solutions (142060.1211, Blooms) and granules of TCP or OCP. The process of 3D printing was as follows. The hydrogel having viscosity 10-29 Pa·s was placed in disposable syringe of 3D printer and then injected through a needle onto the precooled (-20°C) surface with 10% alcohol water (70/30) calcium chloride solution. The printed semi-solid constructs were freeze-dried at -50°C and  $6 \times 10^{-5}$  atm. for 10–12 h. Solidified 3D constructs were washed in distilled water and dried at 37°C for 24h to finalize the synthesis of nonorganic components. The 3D constructs were sterilized by using  $\gamma$ -ray irradiation (15 kGy). The 3D constructs in our tests were represented by cylinders with the 4,0-4,5 diameter and the height of 3-4 mm while weighing 3,5-4,4 mg.

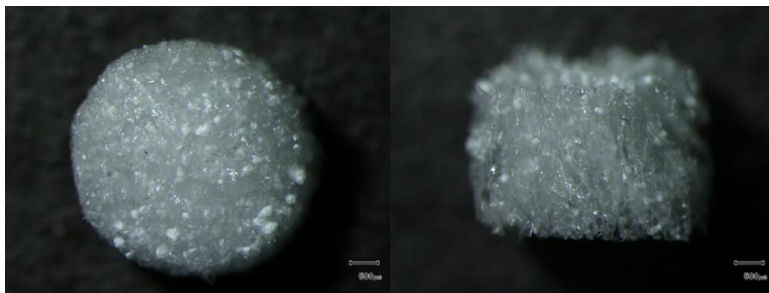


**Figure 1.** The external view of 3D construct based on Alginate-TCP.

### 2.2. Physicochemical analysis

Scanning electron microscope (SEM) Vega II (Tescan, Czech Republic), working in secondary and backscattered electron modes, was used for microstructure studies. The 3D constructs were sputter-coated with a 25 nm thick gold layer prior imaging to impart electrical conductivity of the surfaces.

FTIR spectroscopy was carried out with Nicolet Avatar system (Thermo Fisher Scientific, USA) using the powder mixtures of KBr. Compression testing was carried out using an Instron 4082 testing machine (Bucks, UK) operating at a crosshead speed of 1 mm  $\times$  min<sup>-1</sup>.

### 2.3. Assessment of cytocompatibility and matrix-for-cells property *in vitro*

Cytocompatibility was assessed on a model of human breast osteosarcoma MG-63 cell line (Institute of Cytology of the Russian Academy of Sciences, St Petersburg). The sterilized 3D constructs (sodium alginate + TCP; sodium alginate + OCP) were placed in 96-well culture plate (Costar, USA) in DMEM (PanEco, Russia) supplemented with 10% fetal bovine serum (HyClone, USA) for 3-4 hours till pH achieved 7,0-7,2. After that medium was removed and MG-63 cells at an initial density of  $2 \times 10^4$  cells/cm<sup>2</sup> in 20,0  $\mu$ l of medium were seeded on the surface of the constructs and in the control-wells without constructs, then plates were placed into CO<sub>2</sub>-incubator for 3 hours (37°C, 5 % CO<sub>2</sub>). After that extra 180  $\mu$ l of medium were added in every well and the plates were incubated during 1-14 days. The medium was changed twice a week during the incubation period.

The cellular survival was assessed by using MTT (3-(4,5-dimethylthiazol-2-yl)-2,5-diphenyltetrazolium bromide) assay performed after 1, 3, 7, 10 and 14 days of culture. The amount of

formazan produced by metabolically active viable cells was measured at 550 nm wavelength using a Multiscan microplate reader (ThermoFisher Scientific, USA).

#### *2.4. Biocompatibility assessment of 3D constructs in vivo*

Biocompatibility was estimated on the model of subcutaneous implantation in male BDF1 mice. The grafts were soaked in physiologic saline solution immediately before the surgical procedure. All mice were divided into 3 groups (10 mice per a group) according to the 2 types of grafts: 1st group -sodium alginate -TCP; 2nd group - sodium alginate-OCP. The animals were anesthetized by intraperitoneal injection of mixture ketamine/relanium (1:1) and sterilized 3D constructs were implanted subcutaneously in the back at the level of thoracic spine. The mice were sacrificed at 2, 4, 8 and 12 weeks after implantation (2 mice at a time). The specimens of implanted 3D constructs with adjacent tissues were incised and fixed in 10 % formalin solution, followed by paraffin embedding. Sections (3–4  $\mu\text{m}$ ) were prepared and stained with hematoxylin and eosin (HE) for histological examination. The slides were observed using an Axiovert 40C microscope, and the images were captured by an AxioCam MR3 Camera (both Zeiss, Germany).

#### *2.5. Assessment of osteoplastic properties of 3D constructs*

Osteoplastic properties were investigated on a model of rat tibia fracture. Forty male Wistar rats (180-200 g in weight) were used for this study. The Ethical Committee of P.A. Hertsen Moscow Oncology Research Institute approved the protocol of experiments. The principles of laboratory animal care were followed as in the national laws. The surgical procedures (marginal excision of tibia) were carried out under general anesthesia. The parameters of fracture: 6-8 mm in length, 1,5-2,0 mm in width, 1,5-2,0 in depth. The area of fracture was connected with bone canal which was previously separated from the bone marrow. The 3D constructs of four following types were used: alginate –TCP, alginate –gelatin –TCP, alginate –OCP and alginate –gelatin – OCP. After 3, 6, 9 and 12 weeks after the surgery two rats at a time from each group were sacrificed. The specimen containing the bone graft was fixed with 10% formalin solution for 7 days and then removed calcium using the EDTA solution (0,3 M; 37°C; 25-30 days) after rinsing with distilled water. The paraffinized specimen block was sectioned longitudinally in the center of each defect, and then slides were HE stained for histological examination.

#### *2.6. Statistical analysis*

The results of this study were analysed using standard Student's t-test in Microsoft Excel 2013 Software. Statistical significance was determined at a  $p < 0.05$ .

### **3. Results**

#### *3.1. Scanning electron microscopy (SEM)*

The analysis of SEM-images showed that all four types of 3D constructs had irregular plate-type structure which consisted of alginate with 2-3 mm wide plate, with 500  $\mu\text{m}$  pores between them and with the round shape ceramic granules regardless the type of calcium phosphates. The addition of gelatin to the composition of “ink” did not change the microstructure as well as arrangement and sizes of inner pores (figure 2).

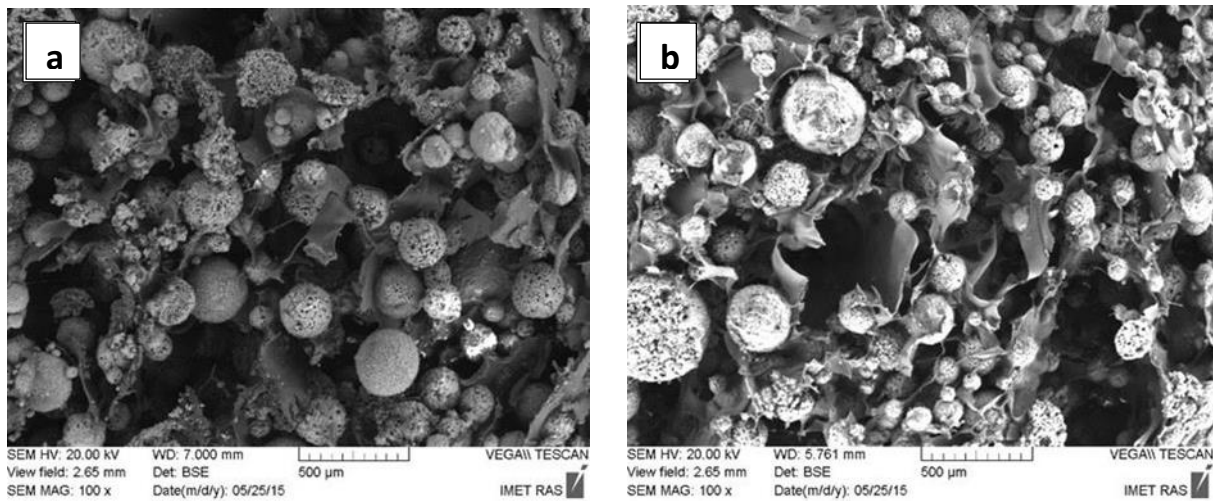


**Figure 2.** SEM images of (a) Alginate-TCP 30 mass %; (b) Alginate-Gelatin(90/10)-TCP 30 mass % (magnification x100).

### 3.2. Component analysis

X-ray phase analysis showed that phase composition of calcium phosphates did not change after addition to the hydrogel and printing of 3D construct. Insignificant decrease of intensity of their peaks determined by alginate content (figure 3).

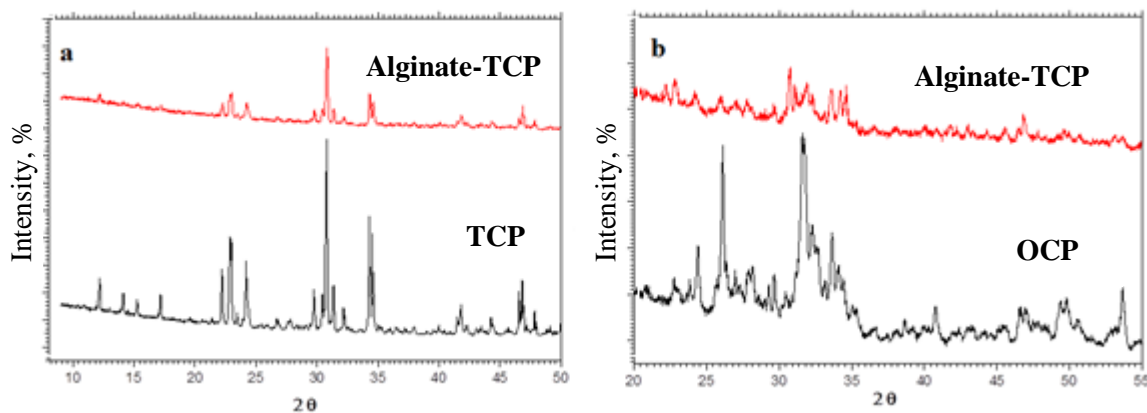


**Figure 3.** The results of X-ray phase analysis of (a) Alginate-TCP composition in comparison to TCP; (b) Alginate-OCP composition in comparison to OCP.

### 3.3. The structure of the 3D constructs

Having taken into the account the fact that following aspects such as efficiency of cells seeding, nutrients and gases delivery, speed of blood vessels growth depend on the porosity of the biomaterial after being implanted in vivo, we paid more attention to the porosity of different compositions. As the result, we could made the conclusion that the decrease of porosity correlated with the increase of calcium phosphate content, 81, 98 % and 63, 92 % for 10 and 30 mass % correspondingly (table 1). Statistically significant increase in pores sizes of 3D constructs based on alginate and 30 mass % TCP was registered after the addition of gelatin in the composition (table 1).

**Table 1.** The structure of 3D printed alginate-TCP-based constructs.

Sample composition	Total porosity of the sample (%), M±s.e.m	Size of inner pores, WxL, µm
Alginate-TCP – 10 mass %	81.98±0.28	400x500
Alginate-TCP – 20 mass %	75.06±0.62	400x500
Alginate-TCP – 30 mass %	63.92±2.33	300x600
Alginate-Gelatin-TCP – 30 mass %	68.23±0.94	600x800

### 3.4. The mechanical properties of 3D constructs

The comparative assessment of mechanical properties of 3D constructs revealed the following: resistance to deformation under compression steadily increased, while the elasticity decreased together with increase of TCP content. The addition of gelatin to the material improved its resistance to deformation under compression (from 3,53±0,39 to 5,28±0,020 MPa) with no practical impact on the elasticity (table 2).

**Table 2.** Mechanical properties of 3D constructs of different composition.

Sample composition	$\sigma^a$ , MPa, M±s.e.m	$\delta^b$ , %, M±s.e.m
Alginate-TCP – 10 mass %	2.71±0.12	15.4±0.16
Alginate-TCP – 20 mass %	3.01±0.13	13.8±0.11
Alginate-TCP – 30 mass %	3.53±0.39	12.4±0.35
Alginate-Gelatin-TCP – 30 mass %	5.28±0.020	12.2±0.16

<sup>a</sup> – resistance to deformation under compression

<sup>b</sup> – elasticity

### 3.5. The results of cytocompatibility assessment

During 2 weeks of culturing an optical density of formazan increased in all experimental groups but the speed of MG-63 cell line proliferation on the different types of 3D constructs differed from each other: for alginate-TCP-based constructs no statistically significant difference from a control group was observed while on the alginate-OCP-based construct cells proliferated more slowly than in a control group.

### 3.6. Analysis of biocompatibility and osteoplastic properties

The biocompatibility properties of 3D constructs we analysed on a model of subcutaneous implantation by means of tissue reactions as well as toxicity and immune cells activity correlated with chemical composition of material. Thus, we assessed the following factors: firstly, the degree of integration of connective-tissue capsule and surrounding tissues as well as its vascularization, secondly, presence/absence of inflammation. There were additional characteristics of biocompatibility such as number of cell layers in the capsule, biodegradation qualities of biomaterial and morphological characteristic of tissue replacing the implanted 3D constructs.

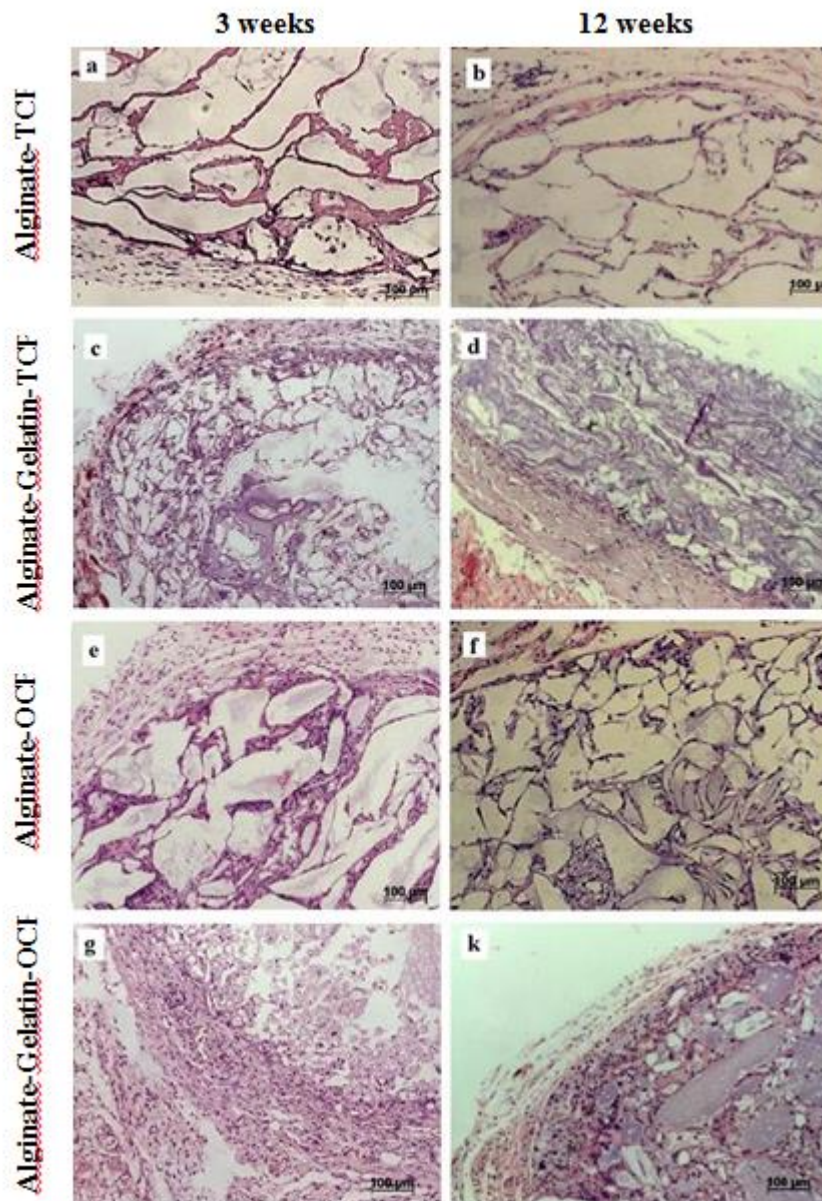


**Figure 4.** Histological sections of the subcutaneously implanted 3D constructs at 2 weeks (a,c,e,g) and 12 weeks (b,d,f,k) after surgery.

**a,b** – Alginate-TCP-based 3D construct; **c,d** – Alginate-Gelatin-TCP-based 3D construct; **e,f** – Alginate-OCP-based 3D construct; **g,k** – Alginate-Gelatin-OCP-based 3D construct. HE, magnification x100.

After subcutaneous implantation of 3D constructs based on Alginate-TCP at early stages (2 weeks after surgery) we observed thin fibrous capsule (up to 8-10 cell layers) with fibers of connective-tissue oriented concentrically and with sprouting small blood capillaries. After the first weeks of implantation we registered active fragmentation of alginate content, and fibroblasts migration to the area of construct. Inner part of constructs was filled with immature connective tissue. 8-12 weeks later the amount of connective tissue inside the implant increased dramatically (figure 4a,b) We observed the appearance of foreign-body giant cells in the newly formed connective tissue together with the reduction of TCP granules which indicated the beginning of biodegradation of the implants. The addition of gelatin to the constructs accelerated these processes which was noticeable at early stages (2 weeks) (figure 4c, d).

The different picture was observed in the situation with OCP-based grafts. At early stages capsule consisted of loose connective tissue with normally oriented fibers, neutrophilic infiltration and active vascularization. 2 weeks after the surgical procedure aseptic inflammation in the area of implantation slowed down. This observation indicated that applied material stimulated the tissue transition from the

inflammation to regeneration. Steady involution of 3D construct with its active replacement by connective tissue with fibroblast-type cells and foreign-body giant cells took place. Relatively small number of blood vessels could be observed (figure 4e, f). It is important to mention that the speed of connective tissue replacement was the maximal when alginate-gelatin-OCP constructs were used (figure 4g, k).

Taken together, experiments *in vivo* demonstrated good biocompatibility for all types of examined 3D constructs. A higher speed of OCP degradation in comparison to TCP was registered as well as faster alginate fragmentation when gelatin was added. All this led to more intensive connective tissue replacement.

Assessment of bone-replacement properties was measured on a model of rat tibia fracture. 3 weeks after the implantation we observed the beginning of alginate layers resorption with its further replacement by fibrous structures with fibroblast-type cells. Sporadic periosteal osteogenesis formations were visualized on the border with healthy bone tissue. Numerous blood vessels were observed throughout the whole area of the cross sections (figure 5a).

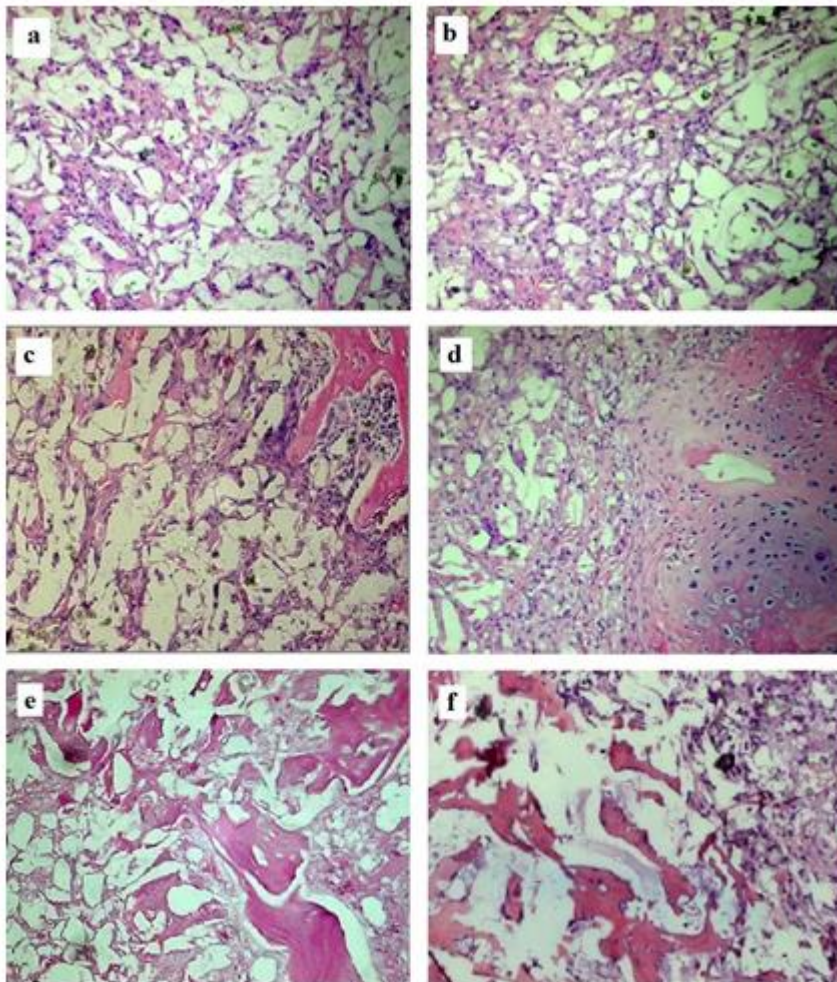


**Figure 5.** Histological sections of Alginate-TCP-based 3D construct (a,b,c) and Alginate-Gelatin-TCP-based 3D construct (d,e,f) in the area of rat tibia fracture.

**a-** 3 weeks after implantation;  
**b** – 6 weeks after implantation; **c** – 9 weeks after implantation;  
**d** – 3 weeks after implantation; **e** – 6 weeks after implantation;  
**f** – 12 weeks after implantation. HE staining, magnification x 100.

After 6 weeks of implantation the fibrous hyperplastic periosteum was observed on the frontier of the fracture. Inside the implant, periosteal osteogenesis was accompanied by endochondral osteogenesis. At the same time, in the area of fracture above thin layer of bone tissue newly formed trabeculae began to appear (figure 5b).

The process of regeneration continued at the late stages of observation. On the one hand, the area of defect was filled with connective tissue, which substituted with spongy bone tissue; on the other hand, granules of TCP were steadily replaced by bone trabecula with hematopoietic loci (fig. 5c). The

addition of gelatin to the composition of 3D constructs did not significantly change the terms and the way of reparative osteogenesis (figure 5 d, e, f).

In case of Alginate-OCP-based 3D constructs implantation, processes of reparative osteogenesis were similar but more intensified: 3 weeks later in the area of defect multicellular fibrous periosteum appeared, the area of fracture was filled with cellular connective tissue, as well as this, on the border with compact bone lower cortical layer we observed newly formed bone tissue trabecula (figure 6a). The newly formed bone tissue trabecula continued to grow together with active bioresorption of OCP granules and osteoclasts accumulation (figure 6b). Direct osteogenesis was also accompanied by endochondral osteogenesis (figure 6c).

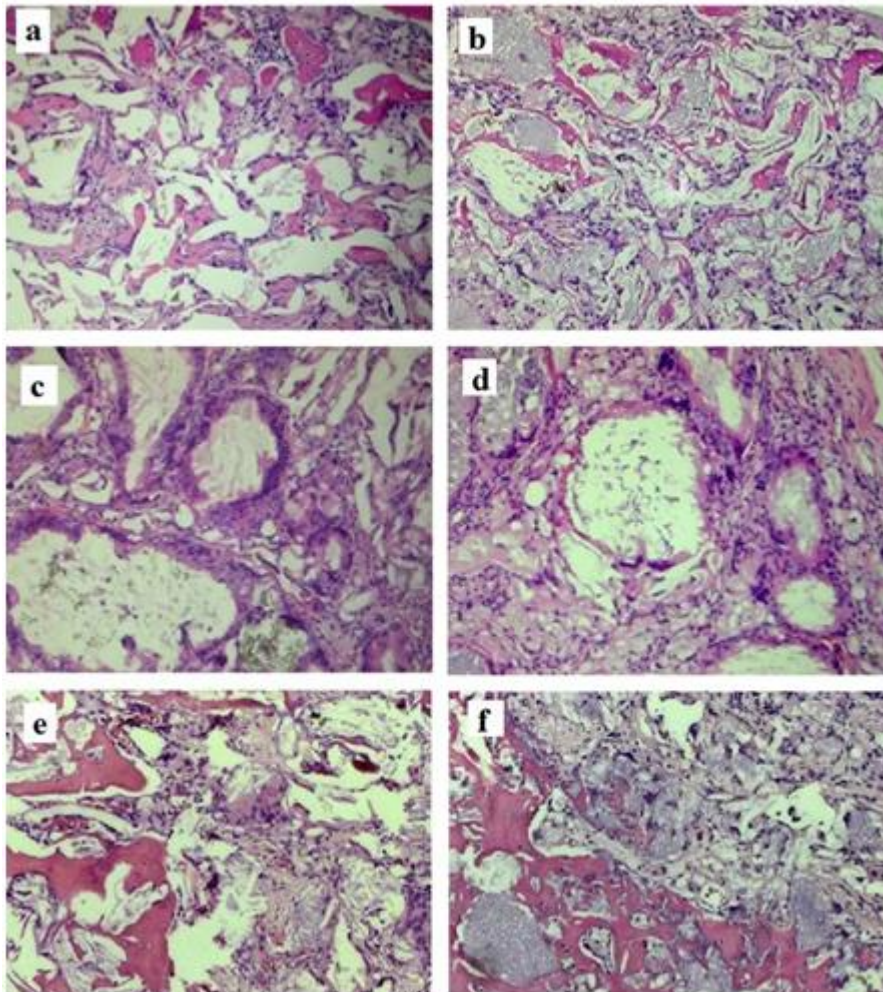


**Figure 6.** Histological sections of Alginate-OCP-based 3D construct (a,b,c) and Alginate-Gelatin-OCP-based 3D construct (d,e,f) in the area of rat tibia fracture.

a- 3 weeks after implantation;  
 b – 6 weeks after implantation;  
 c – 9 weeks after implantation;  
 d – 3 weeks after implantation;  
 e – 6 weeks after implantation;  
 f – 12 weeks after implantation. HE staining, magnification x 100.

The most intensified osteogenesis was observed when the 3-component 3D constructs were used (Alginate-Gelatin-OCP). 3 weeks after the implantation, partly resorbed alginate and gelatin contents were replaced by newly formed connective tissue. The bioresorption of OCP granules also took place which was indicated by the presence of numerous osteoclasts (figure 6 d,e,f). Up to the 12 weeks of observation the newly formed bone tissue trabecula continued to grow (on the frontier of the fracture, as well as, inside the implant) together with the formations of hematopoiesis. The periosteal osteogenesis, as well as, endochondral osteogenesis was observed.

#### 4. Conclusion

In this study, we investigated the mechanical properties, cyto- and biocompatibility, as well as, bone replacement properties of two- and three-component grafts, which were prepared by using 3D printing[8]. Two-component 3D constructs consisted of alginate and one of the two types of calcium

phosphate (TCP or OCP) while three-component 3D constructs additionally included gelatin, which increased their resistance to deformation under compression as well as porosity. The experiments on the model of subcutaneous implantation in mice demonstrated well biocompatibility of all types of 3D constructs. In case of application of OCP-based grafts the highest speed of biodegradation and well-structured connective tissue were observed. The results of implantation of 3D constructs in the rat tibia defects showed the most intensified osteogenesis for the 3-component alginate-gelatin-OCP-based 3D constructs. Thus the results of this study show the feasibility and long-term benefits of applying three-component mineral-polymer composites based on alginate, gelatin and calcium phosphates as osteoplastic materials for printing 3D constructs intended for bone defect replacement.

### References

- [1] Oryan A, Alidadi S *et al.* 2014 *J Orthop Surg Res.* **9** pp 18-42
- [2] Kolk A, Handschel J *et al.* 2012 *J Craniomaxillofac Surg.* **40** pp 706-18
- [3] Pertici G, Carinci F *et al.* 2015 *J Biol Regul Homeost Agents.* **29** (Suppl. 1) pp 136-48
- [4] Komlev V, Barinov S, Bozo I *et al.* 2014 *ACS Appl. Mater. Interfaces.* **6** 16610-20
- [5] Suzuki O, Imaizumi H *et al.* 2008 *Curr. Med. Chem.* **15** 305-13
- [6] Bose S, Vahabzadeh S *et al.* 2013 *Materials Today* **16** pp 496-504